HHS Public Access

Author manuscript

Colloids Surf B Biointerfaces. Author manuscript; available in PMC 2015 December 22.

Published in final edited form as:

Colloids Surf B Biointerfaces. 2014 April 1; 116: 652–657. doi:10.1016/j.colsurfb.2013.10.038.

Mesoporous silica nanoparticles as a breast-cancer targeting ultrasound contrast agent

Andrew Milgroom[a], **Miranda Intrator**[a], **Krishna Madhavan**[a], **Luciano Mazzaro**[a], **Robin Shandas**[a], **Bolin Liu**[b], and **Daewon Park**[a,*]

[a]University of Colorado Denver Anschutz Medical Campus, Department of Bioengineering, Mail Stop 8607, 12700 East 19th Avenue, Aurora, CO 80045, United States

[b]University of Colorado Denver Anschutz Medical Campus, Department of Pathology, Mail Stop 8104, 12801 East 17th Avenue, Aurora, United States

Abstract

Ultrasound (US) is used widely in the context of breast cancer. While it is advantageous for a number of reasons, it has low specificity and requires the use of a contrast agent. Its use as a standalone diagnostic and real-time imaging modality could be achieved by development of a tumor-targeted ultrasound contrast agent (UCA); functionalizing the UCA with a tumor-targeting agent would also allow the targeted administration of anti-cancer drugs at the tumor site. In this article, clinical US techniques are used to show that mesoporous silica nanoparticles (MSNs), functionalized with the monoclonal antibody Herceptin®, can be used as an effective UCA by increasing US image contrast. Furthermore, *in vitro* assays show the successful localization and binding of the MSN-Herceptin conjugate to HER2+ cancer cells, resulting in tumor-specific cytotoxicity. These results demonstrate the potential of MSNs as a stable, biocompatible, and effective therapeutic and diagnostic ("theranostic") agent for US-based breast cancer imaging, diagnosis, and treatment.

Keywords

Mesoporous silica nanoparticles; Ultrasound; Contrast agent; Breast cancer; Drug delivery; Herceptin

1. Introduction

Ultrasound (US) is currently used in breast cancer diagnosis, and for real-time intraoperative localization of breast tumors during resection [1]. While it is relatively low-cost, non-irradiating, and can be monitored in real time, it has low specificity and requires a contrast agent to overcome its inherent noisiness [2]. Development of a targeted ultrasound contrast agent (UCA) would enhance specificity and reduce noise, enabling the use of US as a standalone diagnostic and real-time imaging modality. Current clinically approved UCAs

*Corresponding author at: University of Colorado Denver Anschutz Medical Campus, Department of Bioengineering, Mail Stop 8607, 12700 East 19th Avenue, Aurora, CO 80045, United States. Tel.: +1 303 724 6947; fax: +1 303 724 5800. daewon.park@ucdenver.edu (D. Park).

consist of gas microbubbles encapsulated in protein or liposomal carriers [3]. However, limited bubble half-life (tens of minutes *in vivo*) and instability during insonication diminish their acoustic effectiveness [2]. Mesoporous silica nanoparticles (MSNs) have been shown to stay in the body up to 4 weeks, with peak accumulation in passively targeted reticulo endothelial organs at 24h. [4]. This suggests that tumors passively targeted by MSNs would exhibit a similar peak accumulation time in the body, allowing a much larger time window for UCA use and potentially simplifying clinical procedures. In addition, since all currently approved microbubbles lack the ability to be functionalized with tumor-targeting moieties and are greater than 1 μm in diameter, they are unable to pass through endothelial barriers and accumulate at tumor sites, critically limiting their use as a tumor-targeting agent. Because MSNs are inorganic, solid, and highly porous, they have been the subject of recent studies for use as a long-lasting *in situ* UCA [5–10]. Notably, Liberman et al. have shown gas-filled silica and silica-boron nanoparticles to have a relatively long lifetime *in vivo*, and may be injected up to 24 h. before resection for intraoperative guidance [10]. Liu et al. [5,6], Casciaro et al., [8] and Liu et al. [9] have successfully correlated mean pixel intensity (MPI) and MSN concentration in clinical US ranges, and have reported the successful *in vivo* imaging of MSNs aggregated in the liver.

While use of MSNs as a tumor-targeting UCA has yet to be shown, their role in tumor-targeting drug delivery systems has been explored recently [11].While targeted administration of anti-cancer drugs would be greatly beneficial, the majority of current cytotoxic treatments for breast cancer are not targeted and thus act on off-target sites, resulting in a number of side effects and increasing the risk of secondary cancers [12]. A targeted drug delivery system will reduce the maximum therapeutic dose, as less drug will be released at off-target locations. Boasting low immunogenicity and the ability to be endocytosed by cells, MSNs also allow a high degree of control over loading and release kinetics due to a large functionalizable surface area, high pore volume, and a highly ordered pore structure [13]. Liong et al. [7] have shown preferential uptake of folic acid-conjugated MSNs into PANC-1 and BxPC3 cell lines (pancreatic cancer); the MSNs were then able to release their drug payload into the cytosol, reducing cancer cell survival by 60%. Chen et al. [14] and Meng at al. [15] have demonstrated that MSNs can co-deliver anti-cancer drug and siRNA, thus increasing anti-cancer drug efficacy, mitigating drug resistance *via* the use of siRNA, and reducing systemic drug release prior to MSN delivery to cancer cell. In a related study, Rapoport et al. [16] demonstrated the use of nano/microbubbles for *in vivo* US-induced drug release and imaging; however, this drug delivery system still suffers from short bubble lifetime, and the drug release is dependent on stimulation by US.

We hypothesize that functionalized MSNs can serve as a biocompatible and effective breast cancer-targeting theranostic agent. In this work, we explore this concept using MSNs functionalized with Herceptin®, targeting the human epidermal growth factor receptor 2 (HER2), known to be dysregulated or overexpressed up to 100 fold [17] in certain types of breast cancer. Using conventional clinical US equipment, MSN-Herceptin can confer sufficient MPI to generate high-quality US images. In vitro studies using cells with varying HER2 expression then demonstrate the selectivity of MSN-Herceptin to HER2 overexpressing (HER2+) breast cancer cell lines, and subsequent targeted cell death.

2. Materials and methods

2.1. Materials

MCM-41 type (hexagonal) MSNs, 1N hydrochloric acid, ethanol (200 proof), anhydrous toluene, 1× Phosphate buffered saline (PBS), (3-aminopropyl) triethoxysilane (APTES), dimethylsulfoxide (DMSO), N-hydroxysuccinamide (NHS),1-ethyl-3-(3-dimethylaminopropyl) carbodiimide) (EDC), fluorescein isothiocyanate isomer I (FITC), acrylamide, N, N'-methylene bis(acrylamide) (MBA), ammonium persulfate (APS), and Tetramethylethylenediamine (TMED) were purchased from Sigma–Aldrich (Milwuakee, WI).A1 μm nylon mesh was purchased from Elko Filtration Inc. (Miami, FL). Trastuzumab (Herceptin®) was provided by Dr. Bolin Liu's lab. Dulbecco's Modified Eagle Medium with nutrient mixture F12 (DMEM/F12), fetal bovine serum (FBS) and1% penicillin-streptomycin (PS) were purchased from Invitrogen Inc. (Grand Island, NY).

2.1.1. MSN preparation—MCM-41 MSNs were dispersed in 200 proof ethanol at 5 mg/mL. This dispersion was sonicated for 10 min., vortexing occasionally to maintain suspension, and filtered through nylon mesh (1 μm pore size) from a 10 mL syringe. Retrograde/prograde flow alternation was used to prevent flocculation on the upstream side of the filter. Filtered particles were dried in a 90 °C oven for48 h.

2.2. Determination of acoustic properties

2.2.1. Acoustic measurement apparatus—Single-pulse ultrasound measurements were obtained using non-destructive testing (NDT) transducers with matching frequencies ranging from 0.5 to 7.5 MHz (GE-Panametric™). All transducers were Accuscan type S immersion transducers with point target focus (PTF) and 1-in focus length under water. Two transducers were set facing each other through the round window of a 12″ × 8″ × 3″ acrylic container. An agar cylinder was placed inside and the container was filled with DI water. US gel was applied between the single element transducers and the window. The window was covered in masking tape. Each transducer was designated as a pulser or receiver and attached to a Panametric NDT Model 5800 pulser/receiver. Receiver signal was acquired on an Infiniium 8000 High Performance Oscilloscope (Agilent Technologies™).

2.2.2. Polyacrylamide phantom fabrication—Due to its similarity to soft tissue's acoustic properties [18], acrylamide was selected for the fabrication of the phantom. Polyacrylamide phantoms with varying concentrations of MSNs (0, 0.1, 0.3, 0.5, and 1 mg/mL) were made in triplicate by adding MSNs to 352 μmol acrylamide/35.2 μmol MBA. Prior to polymerization, the solution was sonicated for 3 min. using a probe sonicator. After adding 0.219 μmol APS and 0.219 μmol TMED, 1mL was immediately poured into a 5 mL syringe with the nozzle removed. Complete polymerization occurred between 2–5 min.

2.2.3. Single pulse scan—To quantify the attenuation caused by MSNs, signal loss through polyacrylamide phantoms was measured. Phantoms were placed into acoustic measurement apparatus. 25 μJ pulses were transmitted through the samples at 5kHz. The wave form was averaged and transferred to MATLAB for analysis where attenuation was

calculated using a fast fourier transform (FFT). The FFT was deconvolved with a reference signal of pure water as described by Laugier et al. [19].

2.2.4. B-mode imaging—To correlate image contrast and particle concentration, phantoms were submerged in water on a 5% agar platform, approximately 50 mm in height, to separate the US probe's far-field from the highly reflective bottom of the acoustic measurement apparatus. The phantoms were imaged with a 10MHz probe at 70dB. Two focal points were set at the top and bottom of the phantom, with the top of the phantom 25 mm from the bottom of the phantom. Three images were taken of each phantom. The interior of the phantom's image was parsed into 50×50 pixel squares and measured for MPI. Each square, along with the squares from the other two images of the same concentration, was then averaged. Each mean gray pixel intensity value was correlated to the MSN concentration.

2.2.5. Calculation of axial resolution—Axial resolution was calculated as half of the spatial pulse length (SPL). SPL is defined as the product of the wavelength, λ, and the number of cycles, δ, emitted perpulse. Further, wave length is the ratio of the acoustic velocity, *c*, and the frequency of the incident sound wave, *f*. Here, *f*Y = 7.5 MHz, *c*Y = 1540 m/s, δ = 1, and the axial resolution was be calculated as:

$$R=\frac{\mathrm{SPL}}{2}=\frac{\lambda\times\delta}{2}=\frac{(c/f)\times\delta}{2}=\frac{1540\mathrm{m/s}\times 1}{7.5\times 10^{6}/\mathrm{s}}\times\frac{1}{2}=102.66\mu\mathrm{m} \quad (1)$$

2.3. MSN modification

2.3.1. MSN functionalization—To hydroxylate MSNs (MSN-OH), dried MSNs were resuspended in 10% HCl at 0.5 M stirred for 1h. at room temperature and centrifuged for 5 min. at 5000 rpm. For amine functionalization (MSN-NH_2), 100 mg of MSN-OHs were resuspended in 100 mL of anhydrous toluene. APTES was added to bring the final concentration to 2M and the dispersion was placed in a nitrogen environment. The dispersion was centrifuged for 5 min. at 5000 rpm, decanted, and washed in anhydrous toluene. To purify the particles from unbound APTES, the dispersion was added drop-wise into ether and again centrifuged for 5 min. at 5000 rpm. Centrifugation and wash steps were repeated two more times. After the third decantation, particles were resuspended in 200 proof ethanol and sonicated for 10 min. to reduce aggregation. During sonication the solution was vortexed occasionally to maintain suspension. The particles were dried in a 90 °C oven for 48 h.

2.3.2. MSN conjugation to Herceptin/FITC and FITC—To couple Herceptin to MSNs, amine groups on MSN-NH_2 were conjugated to carboxylates of Herceptin. After preparing a solution of 0.5 mg/mL Herceptin in PBS, 2 mM each of NHS and EDC were added. MSN-NH_2 were suspended in PBS at 4 mg/mL and sonicated for 10 min., then added to the mixture of Herceptin, NHS, and EDC. The EDC coupling reaction was carried out for 4h. under constant stirring at room temperature. The product was then centrifuged for 10 min. at 3000 rpm and decanted to remove the water-soluble carbodiimide and urea by products. The product was resuspended in PBS. The centrifugation, decantation, and

resuspension steps were repeated three times. After the third resuspension to 5 mg/mL in PBS, FITC in DMSO (4mg/mL) was introduced at a ratio of 1:12.5 FITC: Herceptin and allowed to react 1h. with stirring at room temperature in the dark. The solution was dialyzed in 3500 kDa molecular weight cutoff dialysis tubing in milliQ water, carried out at 4 °C in the dark to preserve protein integrity. The water was changed 5 times over a period of 72 h. MSN conjugation to FITC was accomplished in exactly the same manner, replacing Herceptin with FITC, and eliminating the second FITC conjugation. Conjugation efficiencies were determined by analyzing MSN-Herceptin-FITC and MSN-FITC samples using flow cytometry, and are given as the percent of fluorescent particles out of all particles detected.

2.3.3. Determination of MSN size—MSN-NH_2 was prepared as previously described and suspended to a concentration of less than 0.1 mg/mL in PBS (for a particle density of less than 1×10^6 particles/mL). Samples in triplicate were sonicated for 10 and 20 min total, vortexing occasionally to maintain suspension. Particle size distribution was detected using a DPA 4100MFI™ Dynamic Particle Sizer (Bright Well Technologies, Ontario, Canada). Sigma–Aldrich specifies that MSNs have pore volume or $0.98 cm^2$, pore diameter of 2.1–2.7 nm, and surface area of $1000 m^2/g$.

2.4. In vitro studies

2.4.1. Cell culture—For *in vitro* studies, two cell lines with different HER2 expression were used: (1) MDA-MB-231 (TN), which has a very low level HER2 expression (HER2−), and (2) SK-BR-3, which has a moderate level of HER2 expression (HER2+). Both cell lines were cultured in DMEM/F12 with 10% FBS and 1% PS. All cell assays were done in triplicate.

2.4.2. Fluorescence microscopy—To monitor specific binding of the MSN-Herceptin to HER2+ cells, the two cell lines (5×10^4 cells) were cultured with MSN-Herceptin-FITC in 96-well plates. Each cell line was incubated with the MSN-Herceptin-FITC (50 μg/well) for 30 min. The cells were lifted from the well plate by trypsinization. The cell suspension was filtered through an 8 μm nylon mesh filter, allowing free MSN-Herceptin-FITC to pass while trapping MSN-Herceptin-FITC-bound cells on the upstream side. Accumulated cells were detached from the filter by alternating retrograde/prograde flow. Live dead assay was performed using ethidium homodimer-15.1 (EthD-1). These cells were observed under a fluorescent microscope to observe FITC fluorescence as well as the dead cells.

2.4.3. Flow cytometry—Specificity of MSN-Herceptin particles, and conjugation efficiencies of MSN-Herceptin-FITC and MSN-FITC, were quantified using flow cytometry. Cells were prepared in the same manner that was used for fluorescence microscopy. Flow cytometry analysis was performed on a Beckman Coulter Gallios machine (Beckman Coulter, Brea, CA) and data was processed using Kaluza software (Beckman Coulter, Brea, CA).

2.4.4. Ultrasonography—A 2D model was applied to quantitatively demonstrate that cellular uptake of MSNs could augment the inherent contrast in B-mode US images. To

allow uptake of MSNs, the cells are incubated with MSN-Herceptin as previously described for fluorescence microscopy. After incubation, there covered cell suspension was spread across a 10% (wt/v) agar gel. A 50 mm thickness ensured that the focal region of the US beam would not detect reverberations from the plate bottom. Images were acquired as described previously.

3. Results and discussion

3.1. MSNs as an ultrasound contrast agent

Observation of the acoustic properties of non-functionalized MSNs revealed that the backscatter coefficient of these particles is sufficient to be considered as a UCA. For this set of experiments, imaging was limited to a probe with a central frequency of 7.5 MHz with a maximum limit of 10 MHz. Fig. 1 shows the comparison of polyacrylamide phantoms with MCM-41 MSNs at varying concentrations of 0.1 mg/mL (Fig. 1a), 0.3 mg/mL (Fig. 1b), 0.5 mg/mL (Fig. 1c), and 1.0 mg/mL (Fig. 1d). A second-order polynomial was found to fit the data quite well, with an *R*-square value of 0.9764 (Fig. 1e). These images were acquired with 10 MHz probe at a depth of 2.5 cm. With the increase in MSN concentration, one can clearly observe the increase in the contrast. Moreover, MSNs are stable during insonication, indicated by no change in particle size distribution as confirmed by particle size analysis (histograms of particle size distributions can be found in Supplemental Information). Since all MSNs were prepared by initially sonicating for 10 min, the size of particles sonicated for 10 min was compared to the size of particles sonicated for an additional 20 min (30 min total). These two populations were not found to be significantly different (Student's *t*-test, $p = 0.07$). Unfiltered MSN particle sizes were found to have a distribution from 1 to approximately 30 μm, with the majority (95%) having diameter under 10 μm.

The axial resolution (or longitudinal resolution) is defined as the detectable distance between two objects on a line parallel to the direction of wave propagation. The axial resolution was calculated to be 102.66 μm (Eq. (1)), with the MSN diameter close to one hundredth of this. Considering this disparity, creating an image of the individual particle boundary does not cause the apparent contrast. Rather, the apparent contrast is caused by increasing the microscale inhomogeneity of regions *i.e.* MSNs increase the speckle noise within a medium. Although contrast does not reflect the underlying structure of these sub-resolution scatterers, it does reflect their echogenicity [20]. The inherent density and acoustic velocity of MSN in soft tissue yields a substantial degree of reflectivity.

3.2. MSN-cellular interaction

In vitro studies indicate the preferential binding of MSN-Herceptin particles to HER2+ cancer cells. After culture with MSN-FITC and MSN-Herceptin-FITC, both cell populations were sieved using a 10 μm nylon mesh filter, eliminating unbound particles less than 10 μm in diameter. Fluorescence microscopy of HER2+ and HER2− cell lines reveals a detectable difference in interaction with MSN-Herceptin (Fig. 2). While MSN-Herceptin-FITC is present in the filtered HER2− culture, it is primarily unbound, with very few particles attached to the plasma membrane. Conversely, most HER2+ cells show MSN-Herceptin-FITC attachment to the plasma membrane.

The conjugation efficiencies of MSN-Herceptin-FITC and MSN-FITC were determined by flow cytometry, and were found to be 99.47 and 95.83%, respectively. The binding affinity of the nanoparticles was characterized by the relative absorbance near FITC's maximum emission wave length of 520 nm, using a 530/30 band-pass filter. The FITC-conjugated molecules were excited using a 488 nm laser, and polygon-gated to capture the event population with a larger forward and side scatter (Fig. 3). This gating only captures approximately 40% of the event population as a precautionary measure to exclude debris, unbound residual particles, or dead cells. Flow cytometry confirmed binding of MSN-Herceptin-FITC to HER2+ cells and as expected, both control cell populations yielded nearly identical fluorescence. HER2+ cells treated with MSN-Herceptin-FITC showed a strong binding affinity with the nanoparticles (96.2%), while treated HER2− cells exhibited significantly less binding (15.1%). The particle binding to HER2− may be accounted for by a non-amplified level of HER2 expression, or by nonspecific binding due to MSN itself. Indeed, Trewyn et al. [21] have shown that certain cell types naturally incorporate nude MSNs. Furthermore, flow cytometry analysis shows that binding rates of MSN-Herceptin-FITC to HER2+ (SK-BR-3) cells is over twice as high as the binding rate of MSN-FITC alone. The mean binding rates were determined to be 41.59% (SD=19.66%) for MSN-FITC alone, and 89.64% (SD=7.01%) for MSN-Herceptin-FITC. This suggests that Herceptin is indeed an appropriate and effective targeting antibody.

To examine the therapeutic potential of MSN-Herceptin, an MTT cell proliferation assay was not possible since MSN yields a wide absorption spectra and UV/vis spectroscopy was skewed by the concentration of MSNs. Instead, EthD-1was used to determine the ratio of dead cells to total cell count (Fig. 4). By using a 488 nm laser and a 650 nm long pass filter, the tail of the EthD-1emission profile could be observed with minimal overlap from FITC emission spectra. A comparison of the fluorescence of HER2+ cells with and without MSN-Herceptin-FITC treatment suggests that MSN-Herceptin reduces overall cell proliferation, and a shift in fluorescence caused by EthD-1 uptake indicates that the targeting antibody Herceptin maintains a degree of its therapeutic capability. The concentration of MSNs used in cytotoxicity studies remained well under the lethal dose of mesoporous silica, which has been shown to be well over 1 mg/mL [4]. Therefore, it can be deduced that it was indeed the anti-proliferative effects of the targeting antibody Herceptin that induced cell death.

3.3. Diagnostic capability of MSN-Herceptin

HER2+ and HER2− cell lines treated with MSN-Herceptin were assayed for cell surface binding and subjected to US imaging to test the capability of therapeutically-functionalized MSNs to still serve as a UCA. To quantify the peak pixel intensity and thickness of contrast, the pixel intensity profile was graphed (Fig. 5a) along the ordinate indicated by the yellow line in Fig. 5b and c. The presence of MSN-Herceptin results in a spike in contrast by approximately 640%, with a boundary thickness close to 1 mm. Taken together, flow cytometry and *in vitro* US indicate that the preferential binding of MSN-Herceptin particles to the different cell types was significant for cell-specific US contrast enhancement.

4. Conclusion

In this study, we have investigated the *in vitro* targeting and anti-cancer capacity of an MSN-Herceptin system. Using conventional clinical US equipment, MSN-Herceptin was found to confer sufficient MPI generating high-quality US images. *In vitro* studies demonstrated the selectivity of MSN-Herceptin binding to HER2+ breast cancer cell lines, and subsequent cell death. Presently, gas-phase contrast agents are ideal for contrast enhancement in dynamic systems, such as cardiovascular flow, yet MSNs may be more effective in static systems, such as local tumor environments, where they can accumulate in a layer. Antibody-conjugated MSNs are known to stay in the body orders of magnitude longer than the current clinically approved liposome-enclosed air bubbles (days as opposed to minutes), eliminating issues of half-life. Overall, results suggest that MSNs may prove to be a stable, biocompatible, and effective theranostic agent; that is applicable to many other cancers, and quite possibly to other localized conditions.

Supplementary Material

Refer to Web version on PubMed Central for supplementary material.

Acknowledgements

Dr. Donghwa Yun provided instrumental support throughout this project. This work was financially supported by a University of Colorado start-up grant. Dr. Lara Hardesty and Dr. Ann Scherzinger at the University of Colorado Hospital helped with clinical breast cancer diagnostics. Christine Childs at the Colorado Cancer Center Flow Cytometry Shared Resource was instrumental in obtaining flow cytometry results (Cancer Center Support Grant, P30CA046934). Particle sizing was accomplished with help from Dr. John Carpenter's lab in the Skaggs School of Pharmacy and Pharmaceutical Sciences at the University of Colorado Anschutz Medical Campus.

Appendix A. Supplementary data

Supplementary data associated with this article can be found in the online version at http://dx.doi.org/10.1016/j.colsurfb.2013.10.038.

References

1. Blair SL, Thompson K, et al. J. Am. College Surg. 2009; 209:608.
2. Hahn MA, Singh AK, et al. Anal. Bioanal. Chem. 2011; 399:3. [PubMed: 20924568]
3. Doinikov AA, Aired L, et al. Phys. Med. Biol. 2011; 56:6951. [PubMed: 22008736]
4. Liu T, Li L, Teng X, et al. Biomaterials. 2011; 32:1657. [PubMed: 21093905]
5. Liu J, Levine AL, et al. Phys. Med. Biol. 2006; 51:2179. [PubMed: 16625034]
6. Liu J, Li J, Rosol TJ, et al. Phys. Med. Biol. 2007; 52:4739. [PubMed: 17671332]
7. Liong M, Lu J, et al. ACS Nano. 2008; 2:889. [PubMed: 19206485]
8. Casciaro S, Conversano F, et al. Invest. Radiol. 2011; 46:529.
9. Liu YT, Mi Y, Zhao J, et al. Int. J. Pharm. 2011; 421:370. [PubMed: 22001536]
10. Liberman A, Martinez HP, et al. Biomaterials. 2012; 33:5124. [PubMed: 22498299]
11. Mura S, Couvreur P. Adv. Drug Deliv. Rev. 2012; 64:1394. [PubMed: 22728642]
12. Baum M, Buzdar AU, et al. Lancet. 2002; 359:2131. [PubMed: 12090977]
13. Xie M, Shi H, et al. J. Coll. Inter. Sci. 2013; 395:306.
14. Chen AM, Zhang M, et al. Small. 2009; 5:2673. [PubMed: 19780069]
15. Meng HA, Liong M, et al. ACS Nano. 2010; 4:4539. [PubMed: 20731437]

16. Rapoport N, Gao ZG, et al. J. Natl. Cancer Inst. 2007; 99:1095. [PubMed: 17623798]
17. Corsetti V, Houssami N, et al. Eur. J. Cancer. 2008; 44:539. [PubMed: 18267357]
18. Chen X, Novak P, et al. Med. Phys. 2011; 38:1877. [PubMed: 21626921]
19. Laugier P, Droin P, et al. Bone. 1997; 20:157. [PubMed: 9028541]
20. Challis RE, Tebbutt JS, et al. J. Phys. D-Appl. Phys. 1998; 31:3481.
21. Trewyn BG, Nieweg JA, et al. Chem. Eng. J. 2008; 137:23.

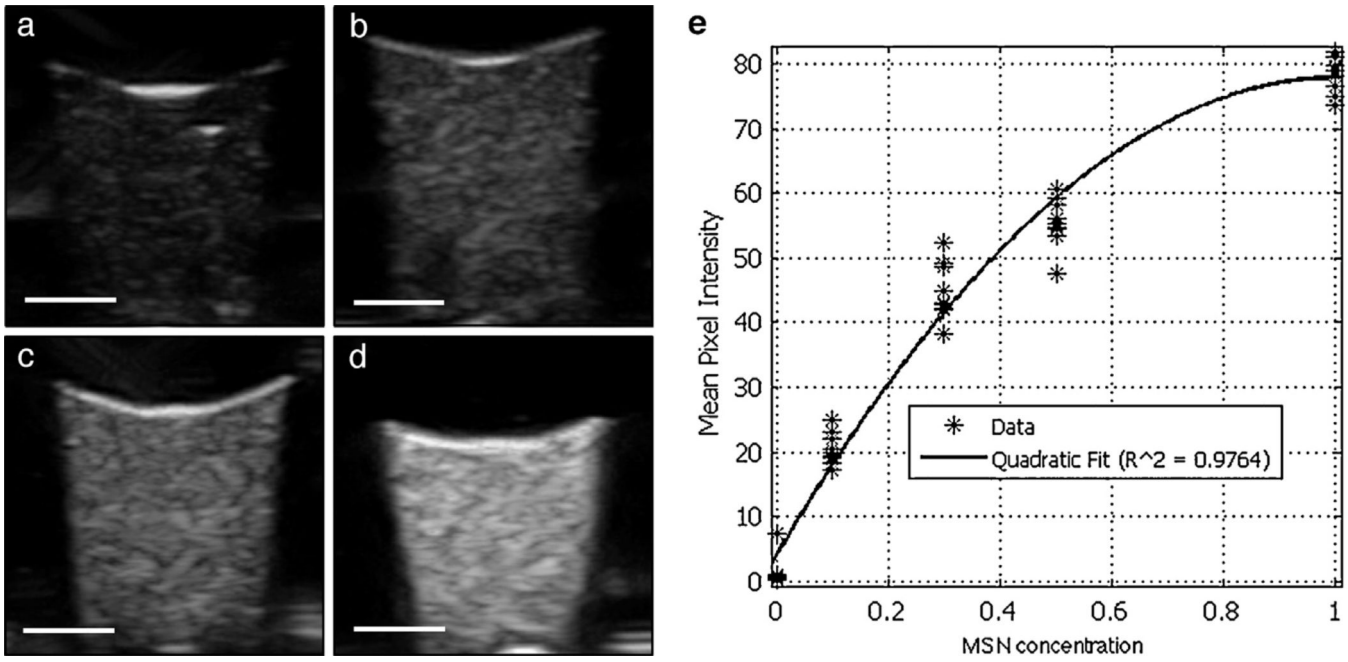

Fig. 1.

Comparison of polyacrylamide phantoms with MCM-41 MSNs at varying concentrations. (a) 0.1 mg/mL, (b) 0.3 mg/mL, (c) 0.5 mg/mL, (d) 1.0 mg/mL, and (e) A quadratic polynomial fits the data well (R^2 = 0.9764). Images acquired with 10 MHz probe at a depth of 3.5 cm. Imaging was limited to a probe with a 7.5 MHz central frequency and 10 MHz maximum limit; exploring higher frequencies was limited by probe type availability. Scale bar:5 mm.

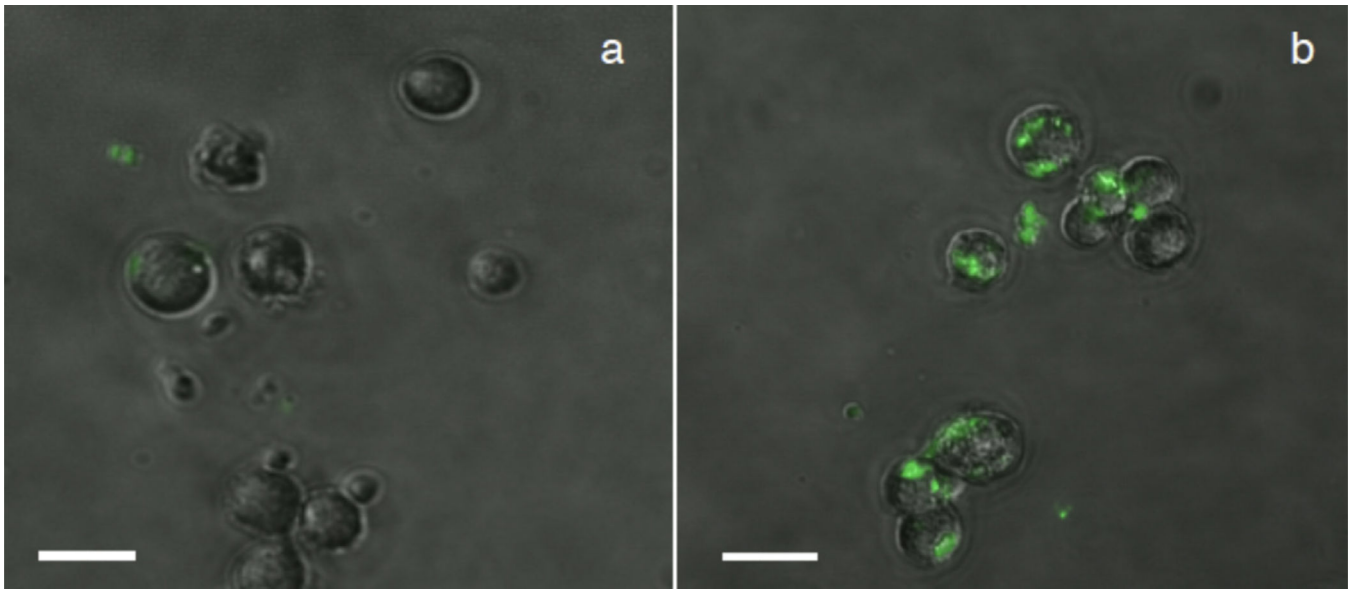

Fig. 2.

Fluorescence microscopy comparison of (a) HER2− (MDA-MB-231) and (b) HER2+ (SK-BR-3) cells treated with MSN-Herceptin-FITC, indicating differential nanoparticle binding and/or internalization to the different cell types. Scale bar: 20 μm.

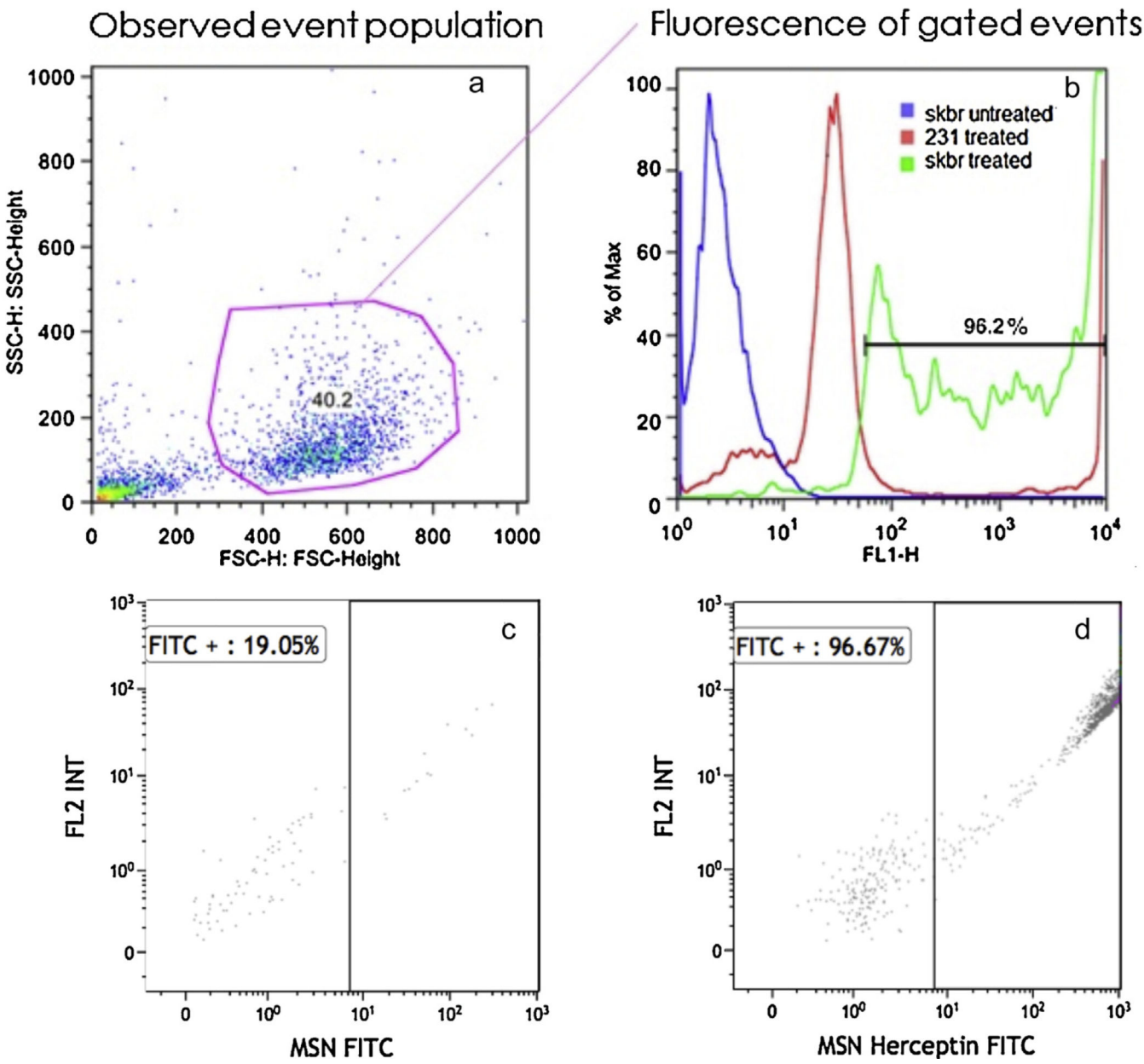

Fig. 3.

Sample gating of cells for flow cytometry. (a) The abscissa represents the forward scatter detector height and the ordinate represents the side scatter detector height. The blue dots represent the HER2+ (SK-BR-3) cells untreated with MSN-Herceptin-FITC, the red dots represent HER2− (MDA-MB-231) cells treated with MSN-Herceptin-FITC and the green dots represent HER2+ (SK-BR-3) cells treated with MSN-Herceptin-FITC, (b) the graph depicts the percentage of absorbance at FITC's maximum emission wavelength of 520 nm, using a 530/30 bandpass filter, (c) representative plot of MSN-FITC binding to HER2+ (SK-BR-3) cells; 19.05%of the particles are bound to the cells, and (d) representative plot of MSN-Herceptin-FITC binding to HER2+ (SK-BR-3) cells; 96.67% of the particles are bound to the cells.

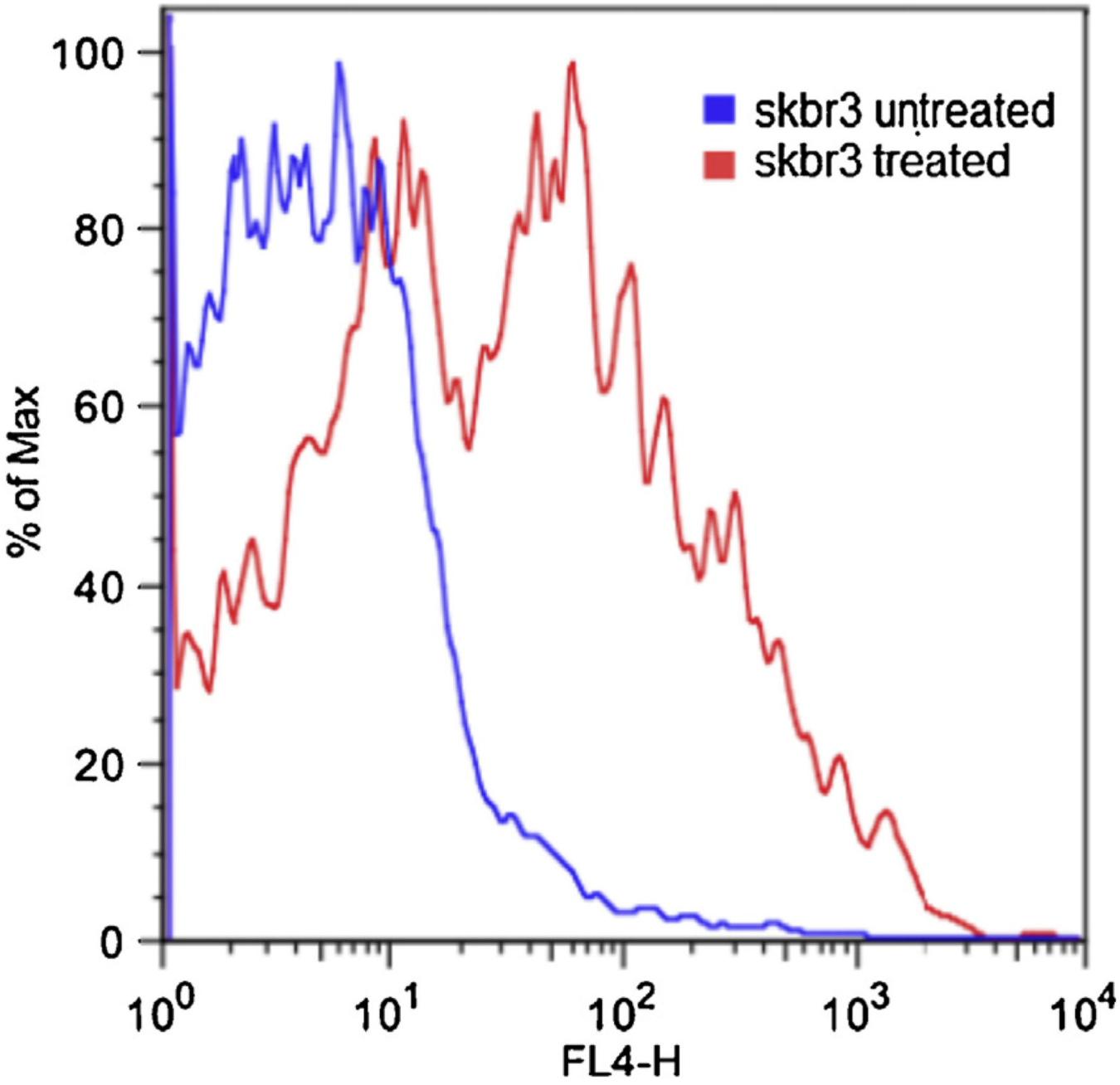

Fig. 4.

Ethidium homodimer-15.1 live/dead assay of HER2+ (SK-BR-3) cells. The blue line indicates the number of dead cells not treated with MSN-Herceptin, and the red line indicates the number of dead cells treated with MSN-Herceptin.

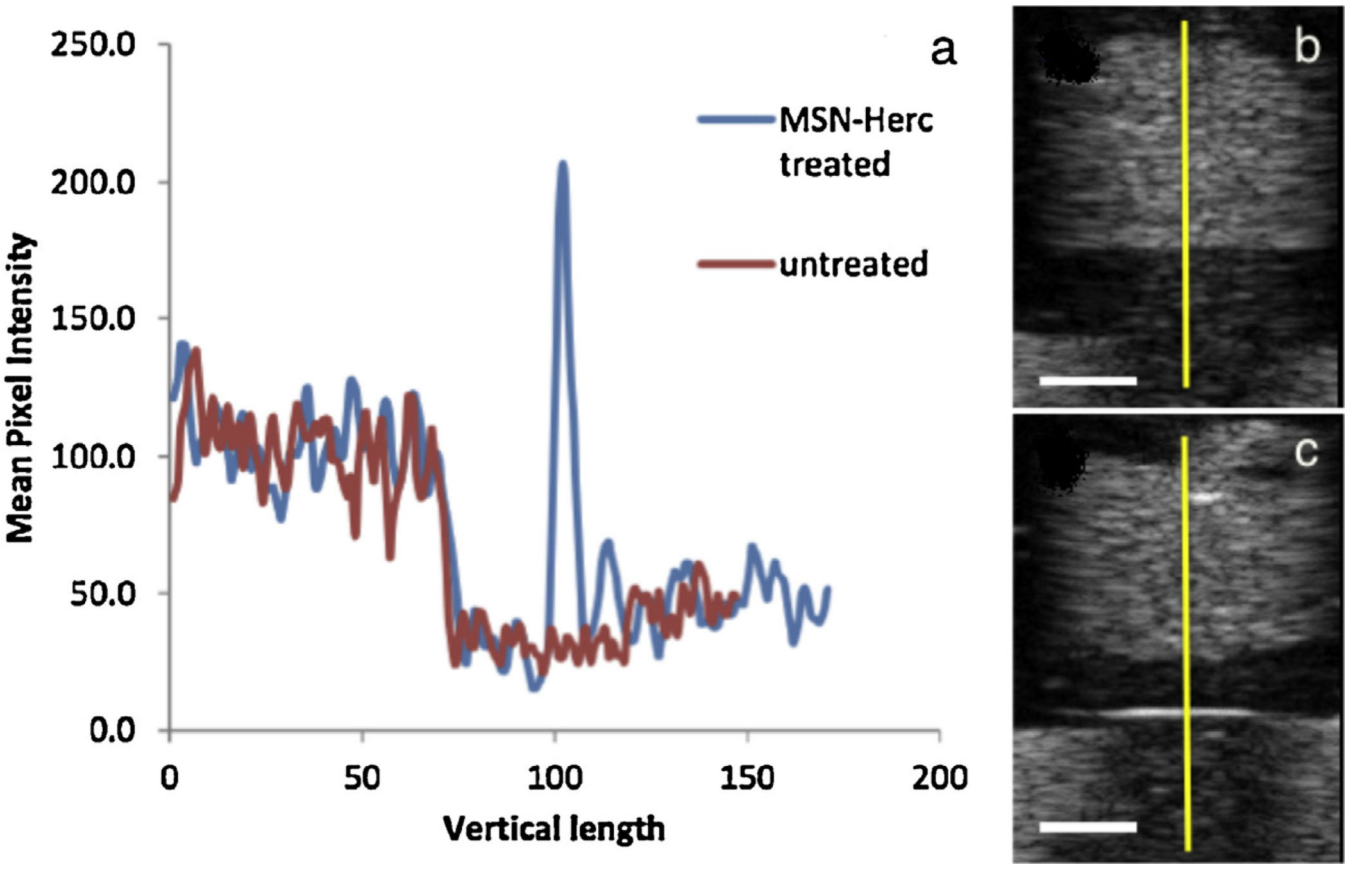

Fig. 5.

(a) Ultrasound contrast profile of (b) HER2+ (SK-BR-3) cells not treated with MSN-Herceptin (red line), and (c) HER2+ cells treated with MSN-Herception (blue line). The pixel intensity profile was graphed along the *y* dimension indicated by the yellow line. Scale bar: 5 mm. (For interpretation of the references to colour in this figure legend, the reader is referred to the web version of this article.)